3 Elastoplastic Problems

3.1 Introduction

There are numerous well−established techniques to calculate effective material characteristics for composite materials. In the case of composite components volume fractions only, one can use the closed form algebraic equations on upper and lower bounds or direct estimates for the effective material tensor components. Otherwise, the cell problems are formulated and solved using their Finite Element Method (FEM) or, alternatively, the Boundary Element Method (BEM) numerical implementations that enable direct computations of the effective characteristics. Recent advances in the area of computational methods in homogenisation of the nonlinear effective characterisation of heterogeneous materials and structures are reported in [4,85,86,107,112,136,250,325]. In the same time, stochastic analysis is still being developed to estimate or to compute probabilistic moments of homogenised material tensors.

Homogenisation of composite materials with elastoplastic constituents is presented below using the so−called Transformation Field Analysis (TFA) proposed by Dvorak and now applied to approximate the effective nonlinear behaviour of a three−component periodic composite. The self−consistent model and Mori−Tanaka theory, providing the estimation of the overall thermoelastic constants of composites on the basis of constituent properties and volume fractions, are partially incorporated in this model. Computational implementation of the method consists of the utilisation of the program ABAQUS to enable automatic homogenisation of n−component periodic composites in a general configuration of the components in the RVE. Numerical examples of the three−component periodic composite homogenisation make it possible to compare the nonlinear behaviour of a composite for its real and homogenised models in the case of the specific boundary problem defined for the cell. The next step in the development of this approach would be to determine the parameter sensitivity of the homogenised properties of the composite with respect to the material characteristics of the constituents as well as to some geometrical data defining the RVE. Statistical and stochastic simulation of probabilistic moments of the effective material tensors would be possible after such a sensitivity determination, taking into account the experimental knowledge of the statistical parameters of the composite constituents.

3.2 Homogenisation Method

The periodic n−component composite in the plane orthogonal to the fibre direction is considered where perfectly bonded components are assumed to be elastoplastic. Mechanical behaviour of the composite constituents is represented by time and temperature dependent constitutive relations under the assumption that for any time τ the total strains and stresses can be decomposed as

$$\varepsilon_r(\mathbf{y},\tau)=\varepsilon_r^{el}(\mathbf{y},\tau)+\varepsilon_r^{*}(\mathbf{y},\tau) \tag{3.1}$$

$$\sigma_r(\mathbf{y},\tau)=\sigma_r^{el}(\mathbf{y},\tau)+\sigma_r^{*}(\mathbf{y},\tau) \tag{3.2}$$

where ε_r^{el}, ε_r^{*} denote elastic strain resulting from a given displacement boundary condition applied on the region Ω_r and the eigenstrain in the same subregion, respectively; σ_r^{el}, σ_r^{*} stand for the elastic stress and eigenstress tensor components in Ω_r. The eigenstrain and eigenstress fields considered here as transformation field may be decomposed in the case of thermal and inelastic effects as

$$\boldsymbol{\varepsilon}_r^{*}(\mathbf{y},\tau)=\mathbf{m}_r\alpha_T(\tau)+\boldsymbol{\varepsilon}_r^{inel}(\mathbf{y},\tau) \tag{3.3}$$

$$\boldsymbol{\sigma}_r^{*}(\mathbf{y},\tau)=\mathbf{l}_r\alpha_T(\tau)+\boldsymbol{\sigma}_r^{rel}(\mathbf{y},\tau) \tag{3.4}$$

where m_r denotes the thermal strain tensor, l_r is the thermal stress tensor, while $\alpha_T(\tau)$ represents the linear thermal expansion coefficient. A procedure of determination of the effective thermal expansion coefficients for various composites has been described in [253,305,311]. Since ε_r^{inel} is the inelastic strain and σ_r^{rel} is the relaxation stress, (3.1) and (3.2) can be written as

$$\varepsilon_r(\mathbf{y},\tau)=\mathbf{M}_r\sigma_r(\mathbf{y},\tau)+\mathbf{m}_r\theta(t)+\varepsilon_r^{inel}(\mathbf{y},\tau) \tag{3.5}$$

$$\sigma_r(\mathbf{y},\tau)=\mathbf{C}_r\varepsilon_r(\mathbf{y},\tau)+\mathbf{l}_r\theta(t)+\sigma_r^{rel}(\mathbf{y},\tau) \tag{3.6}$$

where $\mathbf{C}_r$ and $\mathbf{M}_r$ are the elastic and compliance tensor components for the subregion Ω_r. Hence, it is possible to write the following relations between $\mathbf{m}_r,\mathbf{l}_r,\mathbf{M}_r,\mathbf{C}_r,\varepsilon_r^{inel}$ and σ_r^{rel} :

$$\mathbf{M}_r=\mathbf{C}_r^{-1} \tag{3.7}$$

$$\mathbf{m}_r=-\mathbf{M}_r\mathbf{l}_r \tag{3.8}$$

$$\mathbf{l}_r=-\mathbf{C}_r\mathbf{m}_r \tag{3.9}$$

$$\varepsilon_r^{inel}(\mathbf{y},\tau)=-\mathbf{M}_r\sigma_r^{rel}(\mathbf{y},\tau) \tag{3.10}$$

$$\sigma_r^{rel}(\mathbf{y},\tau)=-\mathbf{C}_r\varepsilon_r^{inel}(\mathbf{y},\tau) \tag{3.11}$$

Mechanical and thermal elastic influence functions are given by the following relations:

$$\varepsilon_r(\mathbf{y},\tau) = \mathbf{A}_r(\mathbf{y})\varepsilon(\tau) + \mathbf{D}_{\mathrm{rs}}(\mathbf{y},\mathbf{y}')\varepsilon_s^*(\mathbf{y},\tau) \tag{3.12}$$

$$\sigma_r(\mathbf{y},\tau) = \mathbf{B}_r(\mathbf{y})\varepsilon(\tau) + \mathbf{F}_{\mathrm{rs}}(\mathbf{y},\mathbf{y}')\sigma_s^*(\mathbf{y},\tau) \tag{3.13}$$

Matrices $\mathbf{B}_r(\mathbf{y})$ and $\mathbf{A}_r(\mathbf{y})$ in (3.12) and (3.13) denote stress and strain concentration factor tensors representing the volume averages of the corresponding functions over the periodicity cell, as is proposed in (3.14) to (3.17). To describe the overall homogenised response of volume Ω, the resulting strains and stresses are combined with their corresponding local components described by (3.3) to (3.6) as

$$\begin{aligned}\varepsilon(\tau) &= \frac{1}{|\Omega|}\int_\Omega \varepsilon_r(\mathbf{y},\tau)d\Omega \\ &= \frac{1}{|\Omega|}\int_\Omega [\varepsilon_{\mathrm{r}}^{\mathrm{el}}(\mathbf{y},\tau) + \varepsilon_{\mathrm{r}}^*(\mathbf{y},\tau)]d\Omega = \varepsilon^{el}(\tau) + \varepsilon^*(\tau)\end{aligned} \tag{3.14}$$

$$\begin{aligned}\sigma(\tau) &= \frac{1}{|\Omega|}\int_V \sigma_r(\mathbf{y},\tau)d\Omega = \\ &\frac{1}{|\Omega|}\int_\Omega [\sigma_{\mathrm{r}}^{\mathrm{el}}(\mathbf{y},\tau) + \sigma_{\mathrm{r}}^*(\mathbf{y},\tau)]d\Omega = \sigma^{el}(\tau) + \sigma^*(\tau)\end{aligned} \tag{3.15}$$

Then, local elastic fields may be written as

$$\varepsilon^{\mathrm{el}}(\tau) = \frac{1}{|\Omega|}\int_\Omega [\mathbf{A}_r(\mathbf{y})\varepsilon(\tau) + \mathbf{a}_r(\mathbf{y})\alpha_T(\tau)]\, d\Omega \tag{3.16}$$

$$\sigma^{el}(\tau) = \frac{1}{|\Omega|}\int_\Omega [\mathbf{B}_r(\mathbf{y})\sigma(\tau) + \mathbf{b}_r(\mathbf{y})\alpha_T(\tau)]\, d\Omega \tag{3.17}$$

where $\mathbf{a}_{\mathrm{r}}(\mathbf{y})$ and $\mathbf{b}_{\mathrm{r}}(\mathbf{y})$ are the thermoelastic strain and stress concentration factors [86,94]. The strain transformation field $\varepsilon^*(\mathbf{y},\tau)$ defined in Ω results in the displacements on the unconstrained part of surface $\partial\Omega$, while the transformation stress $\sigma^*(\mathbf{y},\tau)$ generates surface tractions on Ω being constrained. The relation between the local and global transformation fields is proposed as

$$\varepsilon^*(\tau) = \frac{1}{|\Omega|}\int_\Omega [\varepsilon_r(\mathbf{y},\tau) - \mathbf{A}_r(\mathbf{y})\varepsilon(\tau)]\, d\Omega = \frac{1}{|\Omega|}\int_\Omega \mathbf{A}_r(\mathbf{y})\varepsilon^*(\mathbf{y},\tau)\, d\Omega \tag{3.18}$$

$$\sigma^*(\tau) = \frac{1}{|\Omega|}\int_\Omega [\sigma_{\mathrm{r}}(\mathbf{y}) - \mathbf{B}_r(\mathbf{y})\sigma(\tau)]\, d\Omega = \frac{1}{|\Omega|}\int_V \mathbf{B}_r^T(\mathbf{y})\sigma^*(\mathbf{y},\tau)\, d\Omega \tag{3.19}$$

The elastic local strain $\varepsilon_r(\mathbf{y},\tau)$ and stress fields $\sigma_r(\mathbf{y},\tau)$ are found from a superposition of the elastic local fields $\varepsilon_r^{el}(\mathbf{y},\tau)$ and $\sigma_r^{el}(\mathbf{y},\tau)$ with local eigenstrains $\varepsilon_r^*(\mathbf{y},\tau)$ and eigenstresses $\sigma_r^*(\mathbf{y},\tau)$, respectively; the same model in the context of global scale is introduced analogously. These two different scales are linked using the formulation for local strain and stress fields in the following form:

$$\varepsilon_r(\mathbf{y'}) = \mathbf{A}_r(\mathbf{y'})\varepsilon + \mathbf{D}_{rs}(\mathbf{y},\mathbf{y'})\varepsilon_s^*(\mathbf{y'}) \tag{3.20}$$

$$\sigma_r(\mathbf{y}) = \mathbf{B}_r(\mathbf{y})\sigma + \mathbf{F}_{rs}(\mathbf{y},\mathbf{y'})\sigma_s^*(\mathbf{y'}) \tag{3.21}$$

$\mathbf{D}_{rs}(\mathbf{y},\mathbf{y'})$, $\mathbf{F}_{rs}(\mathbf{y},\mathbf{y'})$ are transformation strain and stress influence functions, which enable us to relate the strain and stress tensor components on the macroscale defined by $\mathbf{y}$ and the microscale identified by $\mathbf{y}'$. Solving the following boundary value problem on the RVE we get

$$div\sigma(\mathbf{y}) = \frac{\partial\sigma(\mathbf{y})}{\partial\mathbf{y}} = 0 \tag{3.22}$$

$$\varepsilon_r(\mathbf{y}) = \mathbf{M}_r\sigma_r(\mathbf{y}) + \varepsilon_r^*(\mathbf{y}) \tag{3.23}$$

$$\frac{1}{|\Omega|}\int_\Omega \varepsilon_r(\mathbf{y})d\Omega = \langle\varepsilon\rangle_\Omega \tag{3.24}$$

$$\mathbf{u}(\mathbf{y}) = \varepsilon\mathbf{y} + \mathbf{u}^*(\mathbf{y}) \tag{3.25}$$

where the local uniform strain field ε_r is found using the matrices $\mathbf{A}_r(\mathbf{y})$, $\mathbf{D}_{rs}(\mathbf{y},\mathbf{y'})$. Further, it is possible to determine the approximated expression of the averaged strain in the subvolume Ω_r given as

$$\varepsilon_r = \mathbf{A}_r\varepsilon + \sum_{r,s=1}^{N}\mathbf{D}_{rs}\varepsilon_r^* \tag{3.26}$$

Analogous to (3.26), the averaged stresses in the subregion Ω_r can be written in the form

$$\sigma_r = \mathbf{B}_r\sigma + \sum_{r,s=1}^{N}\mathbf{F}_{rs}\sigma_r^* \tag{3.27}$$

It is observed that $\mathbf{F}_r(\mathbf{y},\mathbf{y}')$ and $\mathbf{D}_r(\mathbf{y},\mathbf{y}')$ are eigenstress and eigenstrain influence functions, that reflect the effect on the scale **y** resulting from a transformation on the scale **y'** under overall uniform applied stress or strain. The additional influence functions are determined in terms of averages and piecewise constant approximations in the introduced subregions inside the RVE. Therefore, under overall strain $\varepsilon(t)$=0, the transformation concentration factor tensor $\mathbf{D}_{rs}$ gives the strain induced in the subvolume Ω_r by a unit uniform eigenstrain in Ω_s. Under overall stress $\sigma(t)$=0, the concentration factor tensor $\mathbf{F}_{rs}$ defines the stress in Ω_r resulting from the unit eigenstrain located in Ω_s. It can be shown that these tensors can be determined in the case of multiphase medium as

$$\mathbf{D}_{sr} = (\mathbf{I} - \mathbf{A}_r)(\mathbf{C}_r - \mathbf{C})^{-1}(\delta_{rs}\mathbf{I} - \mathbf{c}_s\mathbf{A}_s^T)\mathbf{C}_s \tag{3.28}$$

$$\mathbf{F}_{sr} = (\mathbf{I} - \mathbf{B}_r)(\mathbf{M}_r - \mathbf{M})^{-1}(\delta_{rs}\mathbf{I} - \mathbf{c}_s\mathbf{B}_s^T)\mathbf{M}_s \tag{3.29}$$

(r,s=1,...,N, without summation over repeated indices)

which for a two–component composite gives

$$\begin{aligned}\mathbf{D}_{p\alpha} &= (\mathbf{I} - \mathbf{A}_p)(\mathbf{C}_\alpha - \mathbf{C}_\beta)^{-1}\mathbf{C}_\alpha \\ \mathbf{D}_{p\beta} &= -(\mathbf{I} - \mathbf{A}_p)(\mathbf{C}_\alpha - \mathbf{C}_\beta)^{-1}\mathbf{C}_\beta\end{aligned} \tag{3.30}$$

$$\begin{aligned}\mathbf{F}_{p\alpha} &= (\mathbf{I} - \mathbf{B}_p)(\mathbf{M}_\alpha - \mathbf{M}_\beta)^{-1}\mathbf{M}_\alpha \\ \mathbf{F}_{p\beta} &= -(\mathbf{I} - \mathbf{B}_p)(\mathbf{M}_\alpha - \mathbf{M}_\beta)^{-1}\mathbf{M}_\beta\end{aligned} \tag{3.31}$$

for $p=\alpha,\beta$

This completes the description of the homogenisation method for a composite with elastoplastic coefficients by use of the Transformation Field Analysis (TFA). It should be underlined that, in comparison to the homogenisation model valid for the linear elastic range, the necessity of transformation matrix computations is crucial for the proposed nonlinear FEM analysis.

3.3 Finite Element Equations of Elastoplasticity

The following boundary value problem is now considered [206,210]:

$$\Delta\sigma_{kl,l} = 0\,;\ \mathbf{x}\in\Omega \tag{3.32}$$

$$\Delta\tilde{\sigma}_{kl} = C_{klmn}\Delta\varepsilon_{mn}\,;\ \mathbf{x}\in\Omega \tag{3.33}$$

$$\Delta\varepsilon_{mn} = \tfrac{1}{2}[\Delta u_{k,l} + \Delta u_{l,k} + u_{i,k}\Delta u_{i,l} + \Delta u_{i,k}u_{i,l} + \Delta u_{i,k}\Delta u_{i,l}]\,;\ \mathbf{x}\in\Omega \tag{3.34}$$

with the boundary conditions

$$\Delta\sigma_{\bar{k}l}n_l = \Delta t_{\bar{k}}\,;\ \mathbf{x}\in\partial\,\Omega_\sigma\,,\ \bar{k} = 1,2,3 \tag{3.35}$$

$$\Delta u_{\hat{k}} = \Delta\hat{u}_{\hat{k}}\,;\ \mathbf{x}\in\partial\,\Omega_u\,,\ \hat{k} = 1,2,3 \tag{3.36}$$

This problem is solved for displacements $u_k(\mathbf{x})$, strain $\varepsilon_{kl}(\mathbf{x})$ and stress $\sigma_{kl}(\mathbf{x})$ tensor components fulfilling equilibrium equations (3.32)–(3.36). Let us note that the stress tensor increments $\Delta\sigma_{kl}(\mathbf{x})$, $\Delta\tilde{\sigma}_{kl}(\mathbf{x})$ denote here the first and second Piola–Kirchhoff tensors

$$\Delta\sigma_{kl} = \Delta F_{km}\Delta\tilde{\sigma}_{ml} + F_{km}\Delta\tilde{\sigma}_{ml} + \Delta F_{km}\tilde{\sigma}_{ml}\,;\ \mathbf{x}\in\Omega \tag{3.37}$$

where

$$\Delta F_{km} = \Delta u_{k,m}\,;\ \mathbf{x}\in\Omega \tag{3.38}$$

To get the solution, the following functional defined on the displacement increments as Δu_k is introduced:

$$J(\Delta u_k) = \int_{\Omega}\left(\tfrac{1}{2}C_{klmn}\Delta\varepsilon_{kl}\Delta\varepsilon_{mn} + \tfrac{1}{2}\tilde{\sigma}_{kl}\Delta u_{i,k}\Delta u_{i,l}\right)d\Omega - \int_{\partial\Omega}\Delta\hat{t}_k\Delta u_k d(\partial\,\Omega) \tag{3.39}$$

Let us note that this methodology is common for homogeneous m aterials as well as heterogeneous media. In case of composites, the last equation can be decomposed into the integrals valid for particular constituents and their boundaries and interfaces, separately.

Now, let us introduce the displacement increment function $\Delta u_k(\mathbf{x})$ being continuous and differentiable on Ω and, consequently, including all geometrically continuous and coherent subsets (finite elements) Ω_e, e=1,...,E discretising the entire Ω. It is not assumed that $\Delta u_k(\mathbf{x})$ is differentiable on the interelement surfaces and boundaries $\partial\Omega_{ef}$ (for e,f=1,...,E, $e\neq f$). Next, let us consider the following approximation of $\Delta u_k(\mathbf{x})$ for $\mathbf{x}\in\Omega$:

$$\Delta u_k(\mathbf{x}) = \sum_{\zeta=1}^{N_e}\varphi_{\zeta k}(\mathbf{x})\,\Delta u_{\zeta}^{(N)} \tag{3.40}$$

where $\varphi_{\zeta k}(\mathbf{x})$ are the shape functions for node k, $\Delta u_{\zeta}^{(N)}$ represents the degrees of freedom (DOF) vector, while N_{e} is the total number of the DOF in this node. Considering above, the displacements and strains gradients are rewritten as follows:

$$\Delta u_{k,l}(\mathbf{x}) = \varphi_{k,l}^{\zeta}(\mathbf{x})\,\Delta u_{\zeta}^{(N)} \tag{3.41}$$

$$\Delta\bar{\varepsilon}_{kl}(\mathbf{x}) = [\bar{B}_{kl}^{(1)\zeta} + \bar{B}_{kl}^{(2)\zeta}]\,\Delta u_{\zeta}^{(N)} = \bar{B}_{kl}^{\zeta}\Delta u_{\zeta}^{(N)} \tag{3.42}$$

$$\Delta\bar{\bar{\varepsilon}}_{kl}(\mathbf{x}) = \bar{\bar{B}}_{kl}^{\zeta\xi}\Delta u_{\zeta}^{(N)}\Delta u_{\xi}^{(N)} \tag{3.43}$$

and finally

$$\Delta\varepsilon_{kl}(\mathbf{x}) = \Delta\bar{\varepsilon}_{kl}(\mathbf{x}) + \Delta\bar{\bar{\varepsilon}}_{kl}(\mathbf{x}) \tag{3.44}$$

The following notation is applied (3.42) and (3.43):

$$\bar{B}_{kl}^{(1)\zeta}(\mathbf{x}) = \varphi_{k,l}^{\zeta}(\mathbf{x}) \tag{3.45}$$

$$\bar{B}_{kl}^{(2)\zeta}(\mathbf{x}) = \varphi_{i,k}^{\zeta}(\mathbf{x})\varphi_{i,l}^{\xi}(\mathbf{x})u_{\xi}^{(N)} \tag{3.46}$$

$$\bar{\bar{B}}_{kl}^{\zeta\xi}(\mathbf{x}) = \tfrac{1}{2}\varphi_{i,k}^{\zeta}(\mathbf{x})\varphi_{i,l}^{\xi}(\mathbf{x}) \tag{3.47}$$

All these equations are substituted into the variational formulation of the problem (cf. (3.39)). There holds

$$\begin{aligned}
&\tfrac{1}{2}C_{klmn}\Delta\varepsilon_{kl}\Delta\varepsilon_{mn} = \tfrac{1}{2}C_{klmn}\left(\Delta\bar{\varepsilon}_{kl} + \Delta\bar{\bar{\varepsilon}}_{kl}\right)\left(\Delta\bar{\varepsilon}_{mn} + \Delta\bar{\bar{\varepsilon}}_{mn}\right)\\
&= \tfrac{1}{2}C_{klmn}\left(\Delta\bar{\varepsilon}_{kl}\Delta\bar{\varepsilon}_{mn} + \Delta\bar{\varepsilon}_{kl}\Delta\bar{\bar{\varepsilon}}_{mn} + \Delta\bar{\bar{\varepsilon}}_{kl}\Delta\bar{\varepsilon}_{mn} + \Delta\bar{\bar{\varepsilon}}_{kl}\Delta\bar{\bar{\varepsilon}}_{mn}\right)\\
&= \tfrac{1}{2}C_{klmn}\Big(\bar{B}_{kl}^{\zeta}\Delta u_{\zeta}^{(N)}\bar{B}_{mn}^{\xi}\Delta u_{\xi}^{(N)} + \bar{B}_{kl}^{\zeta}\Delta u_{\zeta}^{(N)}\bar{\bar{B}}_{mn}^{\mu\nu}\Delta u_{\mu}^{(N)}\Delta u_{\nu}^{(N)}\\
&+ \bar{\bar{B}}_{kl}^{\zeta\xi}\Delta u_{\zeta}^{(N)}\Delta u_{\xi}^{(N)}\bar{B}_{mn}^{\mu}\Delta u_{\mu}^{(N)} + \bar{\bar{B}}_{kl}^{\zeta\xi}\Delta u_{\zeta}^{(N)}\Delta u_{\zeta}^{(N)}\bar{\bar{B}}_{mn}^{\mu\nu}\Delta u_{\mu}^{(N)}\Delta u_{\nu}^{(N)}\Big)
\end{aligned} \tag{3.48}$$

$$\tfrac{1}{2}\tilde{\sigma}_{kl}\Delta u_{i,k}\Delta u_{i,l} = \tfrac{1}{2}\tilde{\sigma}_{kl}\varphi_{i,k}^{\zeta}(\mathbf{x})\Delta u_{\zeta}^{(N)}\varphi_{i,l}^{\xi}(\mathbf{x})\Delta u_{\xi}^{(N)} \tag{3.49}$$

Next, the following notation is applied:

$$k_{\zeta\xi}^{(\sigma)e} = \int_{\Omega_e}\tilde{\sigma}_{kl}\varphi_{i,k}^{\zeta}(\mathbf{x})u_{\zeta}^{(N)}\varphi_{i,l}^{\xi}(\mathbf{x})\,d\Omega \tag{3.50}$$

$$k_{\zeta\xi}^{(con)e} = \int_{\Omega_e}\tfrac{1}{2}C_{klmn}\bar{B}_{kl}^{(1)\zeta}\bar{B}_{mn}^{(1)\xi}\,d\Omega \tag{3.51}$$

$$k_{\zeta\xi}^{(u)e} = \int_{\Omega_e}\tfrac{1}{2}C_{klmn}\left(\bar{B}_{kl}^{(1)\zeta}\bar{B}_{mn}^{(2)\xi} + \bar{B}_{kl}^{(2)\zeta}\bar{B}_{mn}^{(1)\xi} + \bar{B}_{kl}^{(2)\zeta}\bar{B}_{mn}^{(2)\xi}\right)d\Omega \tag{3.52}$$

where

$$k_{\zeta\xi}^{(1)e} = k_{\zeta\xi}^{(\sigma)e} + k_{\zeta\xi}^{(con)e} + k_{\zeta\xi}^{(u)e} \tag{3.53}$$

and for the second and third order terms

$$k^{(2)e}_{\zeta\xi} = \int_{\Omega_e} \tfrac{3}{2} C_{klmn} \left(\overline{B}^{\zeta}_{kl} \Delta u^{(N)}_{\zeta} \overline{\overline{B}}^{\mu\nu}_{mn} \Delta u^{(N)}_{\mu} \Delta u^{(N)}_{\nu} + \overline{\overline{B}}^{\zeta\xi}_{kl} \Delta u^{(N)}_{\zeta} \Delta u^{(N)}_{\xi} \overline{B}^{\mu}_{mn} \Delta u^{(N)}_{\mu} \right) d\Omega \tag{3.54}$$

$$k^{(3)e}_{\zeta\xi} = \int_{\Omega_e} 2C_{klmn} \left(\overline{\overline{B}}^{\zeta\xi}_{kl} \Delta u^{(N)}_{\zeta} \Delta u^{(N)}_{\xi} \overline{\overline{B}}^{\mu\nu}_{mn} \Delta u^{(N)}_{\mu} \Delta u^{(N)}_{\nu} \right) d\Omega \tag{3.55}$$

Introducing $k^{(i)}_{\zeta\xi}$ for i=1,2,3 to the functional $J(\Delta u_k)$ in (3.39) and applying the transformation from the local to the global system by the use of the following formula, typical for the FEM implementation:

$$\Delta u^{(N)}_{\zeta} = a_{\xi\alpha} \Delta q_{\alpha} \tag{3.56}$$

it is obtained that

$$\begin{aligned} J(\Delta q_{\alpha}) &= \tfrac{1}{2} K^{(1)}_{\alpha\beta} \Delta q_{\alpha} \Delta q_{\beta} + \tfrac{1}{3} K^{(2)}_{\alpha\beta\gamma} \Delta q_{\alpha} \Delta q_{\beta} \Delta q_{\gamma} \\ &+ \tfrac{1}{4} K^{(3)}_{\alpha\beta\gamma\delta} \Delta q_{\alpha} \Delta q_{\beta} \Delta q_{\gamma} \Delta q_{\delta} - \Delta Q_{\alpha} \Delta q_{\alpha} \end{aligned} \tag{3.57}$$

The stationarity of the functional $J(\Delta q_{\alpha})$ leads to the following algebraic equation:

$$K^{(1)}_{\alpha\beta} \Delta q_{\beta} + K^{(2)}_{\alpha\beta\gamma} \Delta q_{\beta} \Delta q_{\gamma} + K^{(3)}_{\alpha\beta\gamma\delta} \Delta q_{\beta} \Delta q_{\gamma} \Delta q_{\delta} = \Delta Q_{\alpha} \tag{3.58}$$

being fulfilled for any configuration of **Ω**. The iterative numerical solution of this equation makes it possible, according to the specified boundary conditions, to compute the effective constitutive tensor components of the homogenised composite. It should be stressed that the first two components of the stiffness matrix are considered only in further numerical analysis (geometrical nonlinearity is omitted in the homogenisation process); a detailed description of the numerical integration and solution of (3.58) can be found in [12,72,271,276], for instance.

3.4 Numerical Analysis

As was mentioned above, the main goal of the TFA approach is to compute the transformation matrices $\mathbf{A}_r$, $\mathbf{D}_{rs}$ that are determined only once for the original geometry of the composite and assuming initially linear elastic characteristics of the constituents. There holds that

$$\langle d\sigma_r \rangle_{\Omega_r} = \mathbf{C}^{\mathrm{eff}}_{\mathrm{r}} \langle \mathrm{d}\varepsilon_{\mathrm{r}} \rangle_{\Omega_r} = \mathbf{C}^{\mathrm{eff}}_{\mathrm{r}} \langle (d\varepsilon^{el}_r + d\varepsilon^{\mathrm{inel}}_{\mathrm{r}}) \rangle_{\Omega_r}$$

$$\left\langle d\varepsilon_r \right\rangle_{\Omega_r} = \mathbf{A}_\mathrm{r} d\varepsilon + \sum_{r,s=1}^{\mathbf{N}} \mathbf{D}_{\mathrm{rs}} \left\langle d\varepsilon_\mathrm{s}^{\mathrm{inel}} \right\rangle_{\Omega_s} \tag{3.59}$$

$$\left\langle d\boldsymbol{\sigma}_r^{el} \right\rangle_{\Omega_r} = \mathbf{C}_\mathrm{r}^{\mathrm{el}} \left\langle d\boldsymbol{\varepsilon}_r^{el} \right\rangle_{\Omega_r} \text{ and } \left\langle d\boldsymbol{\sigma}_r^{inel} \right\rangle_{\Omega_r} = \mathbf{C}_\mathrm{r} \left\langle d\boldsymbol{\varepsilon}_r^{inel} \right\rangle_{\Omega_r} \tag{3.60}$$

$$\mathbf{C}_\mathrm{r}^{\mathrm{eff}} = \mathbf{C}_r^{el} + \mathbf{C}_r \tag{3.61}$$

Further, using spatial averaging definitions, the averaged stress tensor components are calculated as follows:

$$\left\langle \varepsilon_r \right\rangle_{\Omega} = \varepsilon \text{ and } \left\langle \sigma_\mathrm{r} \right\rangle_{\Omega} = \sigma \tag{3.62}$$

Hence, the effective elasticity tensor components $\mathbf{C}^{eff}$ are derived for a given increment as

$$d\sigma = \mathbf{C}^{eff} \mathrm{d}\varepsilon \tag{3.63}$$

$$\mathbf{C}^{eff} = \sum_{r=1}^{N} c_r \mathbf{C}_r^{el} + \sum_{r,s=1}^{N} \mathrm{c}_\mathrm{r} \left(\mathbf{D}_{rs} \boldsymbol{\varepsilon}_\mathrm{s}^{inel}\right)^{-1} : \boldsymbol{\sigma}_r^{inel} \tag{3.64}$$

In the particular case of a two−component composite, the transformation and concentration matrices are obtained as, cf. (3.30) and (3.31)

$$\mathbf{D}_{11} = (\mathbf{I} - \mathbf{A}_1)(\mathbf{C}_1 - \mathbf{C}_2)^{-1}\mathbf{C}_1 \tag{3.65}$$

$$\mathbf{D}_{21} = (\mathbf{I} - \mathbf{A}_2)(\mathbf{C}_1 - \mathbf{C}_2)^{-1}\mathbf{C}_1 \tag{3.66}$$

$$\mathbf{D}_{12} = -(\mathbf{I} - \mathbf{A}_1)(\mathbf{C}_1 - \mathbf{C}_2)^{-1}\mathbf{C}_2 \tag{3.67}$$

$$\mathbf{D}_{22} = -(\mathbf{I} - \mathbf{A}_2)(\mathbf{C}_1 - \mathbf{C}_2)^{-1}\mathbf{C}_2 \tag{3.68}$$

$\mathbf{C}_1, \mathbf{C}_2$ denote here the components corresponding to elastic properties, while $\mathbf{A}_1, \mathbf{A}_2$ are mechanical concentration matrices. Finally, using (3.64) it is obtained that

$$\begin{aligned} \mathbf{C}^{eff} = \sum_{r=2}^{N} c_1 \mathbf{C}_1^{el} + c_2 \mathbf{C}_2^{el} + \sum \mathrm{c}_1 \left(\mathbf{D}_{11} \varepsilon_1^{inel}\right)^{-1} : \sigma_1^{inel} + \mathrm{c}_2 \left(\mathbf{D}_{12} \varepsilon_2^{inel}\right)^{-1} : \sigma_2^{inel} \\ + \sum \mathrm{c}_1 \left(\mathbf{D}_{21} \varepsilon_1^{inel}\right)^{-1} : \sigma_1^{inel} + \mathrm{c}_2 \left(\mathbf{D}_{22} \varepsilon_2^{inel}\right)^{-1} : \sigma_2^{inel} \end{aligned} \tag{3.69}$$

The FEM aspects of TFA computational implementation are discussed in detail in Section 3.4 below. Further, it should be noticed that there were some approaches in the elastoplastic approach to composites where, analogously to the linear elasticity homogenisation method, the approximation of the effective yield limit stresses of a composite is proposed as a quite simple closed form function

$$\sigma^{(eff)} = \sqrt{\sigma_1 \sigma_2} \tag{3.70}$$

or, in terms of the effective yield surface, in the following form:

$$\Phi(\sigma) = \max_{y \geq 0} \left\{ \left[c_2 + c_1 \left(\frac{\sigma_y^{(1)}}{\sigma_y^{(2)}} \right) y \right]^{-1} \sigma \left[m(y)\sigma - \left(\sigma_y^{(2)} \right)^2 \right] \right\} \tag{3.71}$$

where $m(y = \frac{\mu_1}{\mu_2}) = 3\ \mu_2 V(\mu_1, \mu_2)$ and V is any estimate of the viscosity compliance tensor defined using the viscosities μ_1 and μ_2. A review of the most recent theories in this field can be found in [381], for instance.

The main aim of computational experiment presented is to determine the global nonlinear homogenised constitutive law for two component composites with elastoplastic components; the FEM based program ABAQUS [1] is used in all computational procedures. However the method presented can be implemented in any nonlinear FEM plane strain/stress code such as [60], for instance. The numerical experiments are carried out in the microstructural (RVE) level, and that is why the global response of the composite is predicted starting from the behaviour of the periodicity cell. The numerical micromechanical model consists of a three−component periodicity cell with horizontal and vertical symmetry axes and dimensions 3.0 cm (horizontal) × 2.13 cm (vertical) (cf. Figure 3.1 and 3.2). The composite is made of epoxy matrix and metal reinforcement with material properties of the components collected in Table 1. The void embedded into the steel casting simulates a lack of any matrix in the periodicity cell. Some nonzero material data are introduced to avoid numerical singularities during the homogenisation problem solution.

The 10−node biquadratic, quadrilateral hybrid linear pressure reduced integration plane strain finite elements with 4 integration Gaussian points are used to discretise the cell. Periodic boundary conditions are imposed to ensure periodic character of the entire structure behaviour. A suitable formulation of displacement boundary conditions has the following form:

$$u_i = \varepsilon_{ij} (y(P_2) - y(P_1)) \tag{3.72}$$

where $u_i = \{u_1, u_2\}$ represents the displacement function components, ε_{ij} is the global total strain imposed on the periodicity cell, while $y(P_1)$ and $y(P_2)$ denote coordinates of the points lying on the opposite sides of the RVE.

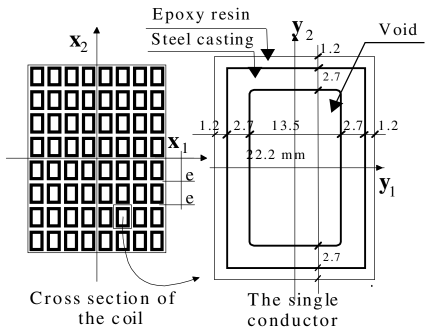

Figure 3.1. Cross section of a superconducting coil

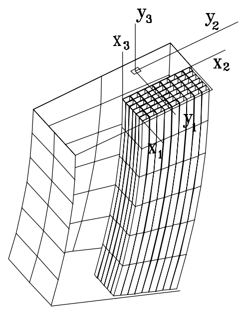

Figure 3.2. 3D view of the superconducting coil part

Table 3.1. Material characteristics of composite constituents

No	Material	Young modulus	Poisson ratio	Yield stress
1	Epoxy resin	7000.0	0.3	10.0
2	Metal	42000.0	0.2	22.0
3	Void	70.0	0.1	0.1

To calculate the effective tensor components, the boundary value problem given by (3.22) − (3.25) is solved first, where the periodicity cell is discretised with 25 finite elements of the type CGPE10R implemtented into the system ABAQUS. The displacement boundary conditions are introduced at the edges of the RVE quarter as is shown in Figures 3.3 and 3.4.

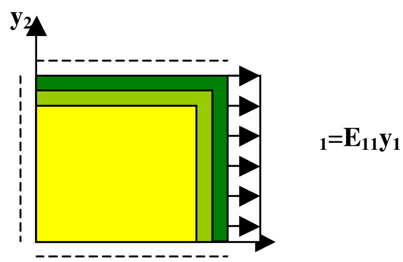

Figure 3.3. Boundary conditions for $E_{11} \neq 0$

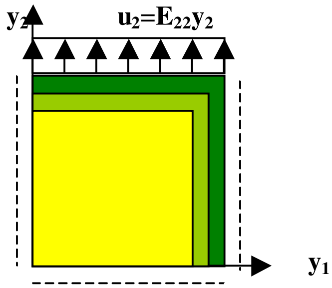

Figure 3.4. Boundary conditions for $E_{22} \neq 0$

Further, since the generalised plane strain is considered, the matrices computed have a rank $\alpha = 4$ and the total dimensions of the matrices $\mathbf{A}_r$ and $\mathbf{D}_{rs}$ are $[4 \times 4]$. The first step in the numerical analysis is to compute mechanical and transformation concentration matrices $\mathbf{A}_r$ and $\mathbf{D}_{rs}$, which is carried out according to the special purpose implementation in the computer system ABAQUS. Transformation matrices $\mathbf{A}_r$ and $\mathbf{D}_{rs}$ are evaluated as

(1) matrix $\mathbf{A}_r$ by means of the overall strain loading case $\varepsilon = \{\varepsilon_{ij}\} = [\varepsilon_{11}, \varepsilon_{22}, 2\varepsilon_{12}, \varepsilon_{33}]^T$ introduced using displacements

$$u_i = \varepsilon_{ij} y_j , \tag{3.73}$$

(2) matrix $\mathbf{D}_{rs}$ imposing the uniform eigenstrain in the subvolume V_r or V_s as the uniform stress; since it is not possible to introduce the eigenstrain directly in each subvolume in the program ABAQUS, the stress tensor components are calculated as

$$\sigma_r^* = -\mathbf{C}_r : \varepsilon_r^* \text{, and } r=1,...,N \tag{3.74}$$

and imposed on each of the N subvolumes, where the elasticity tensor $\mathbf{C}_r$ is given by

$$\mathbf{C}_r = \frac{E_r}{(1-\nu_r)(1-2\nu_r)} \begin{bmatrix} 1-\nu_r & \nu_r & \nu_r & 0 \\ \nu_r & 1-\nu_r & \nu_r & 0 \\ \nu_r & \nu_r & 1-\nu_r & 0 \\ 0 & 0 & 0 & \frac{1-2\nu_r}{2} \end{bmatrix} \tag{3.75}$$

The accuracy of the homogenisation method applied for a given material model is verified by comparison with the results obtained for real heterogeneous composite under the same boundary conditions. For this purpose, the same boundary value problem is solved with four different loading cases. The elastoplastic static analysis consists of 25 incremental load steps (with a constant increment in each step) and is performed using the Radial Return algorithm for the perfect J_2 elastoplastic material. The results in the form of stress strain relations are shown in Figures 3.5 to 3.8, while the stress distribution in the periodicity cell can be compared in Figures 3.9 to 3.12.

Generally, it is observed that the elastic range is very well approximated by the TFA model results. However, the homogenised material seems to be a little stiffer than the heterogeneous one, especially in the nonlinear range in the direction y_1 of the RVE. At the same time, for the interrelation of shear strain and stress, the last incremental steps show almost linear behaviour and that is why practically there is no difference between heterogeneous and homogeneous material. To obtain more efficient effective elastoplastic properties, homogenisation method presented above should be corrected to include the increments of transformation matrices during the loading process.

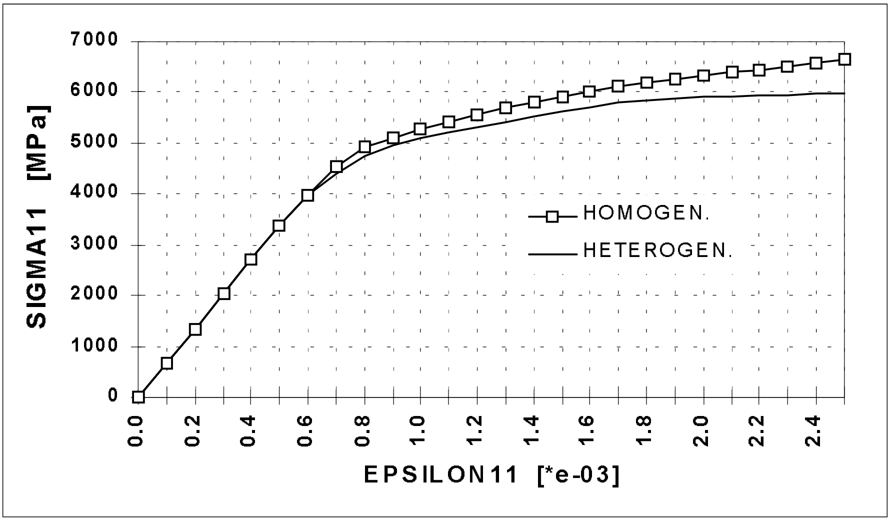

Figure 3.5. Constitutive σ_{11}-ε_{11} relation for homogenised and real composites

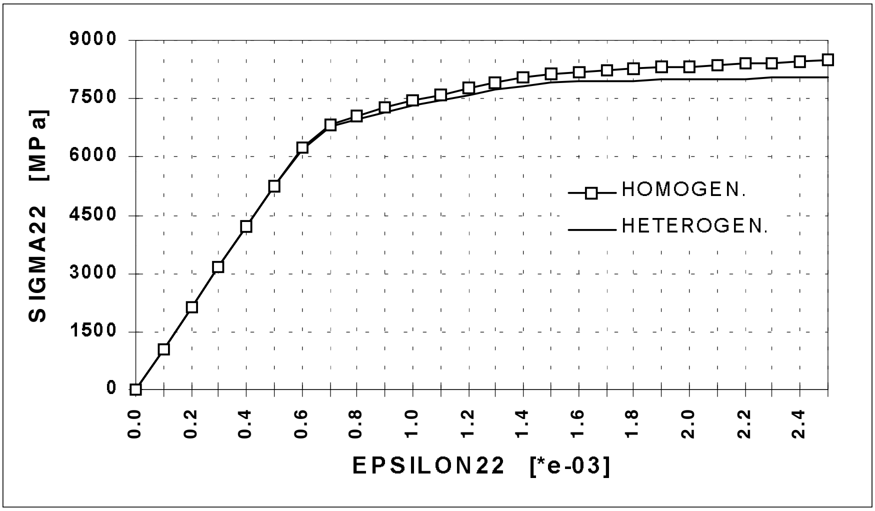

Figure 3.6. Constitutive σ_{22}-ε_{22} relation for homogenised and real composites

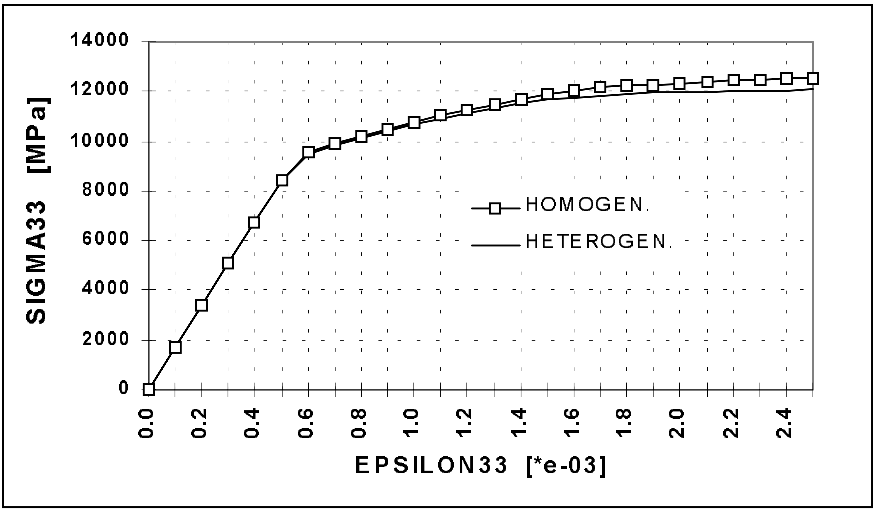

Figure 3.7. Constitutive σ_{33}-ε_{33} relation for homogenised and real composites

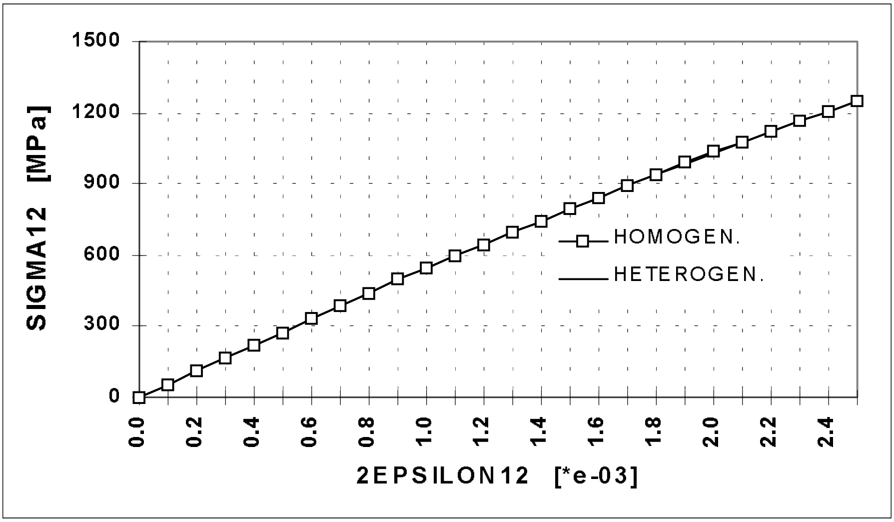

Figure 3.8. Constitutive σ_{12}-$2\varepsilon_{12}$ relation for homogenised and real composites

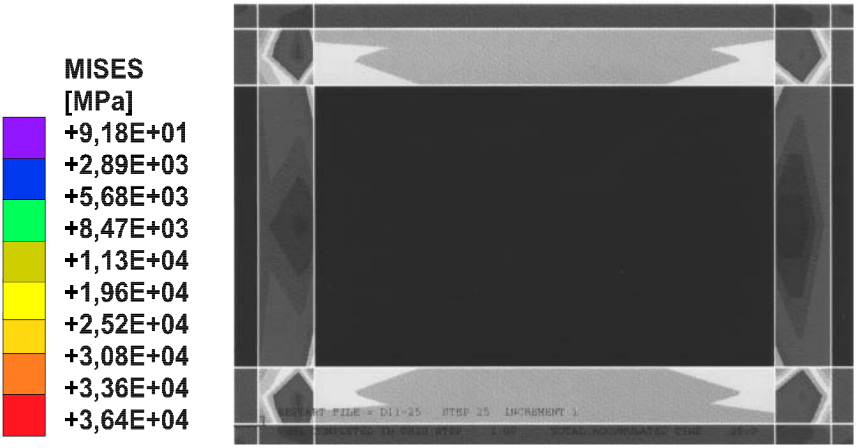

Figure 3.9. The equivalent stress σ_{11}^{eq} distribution in the RVE

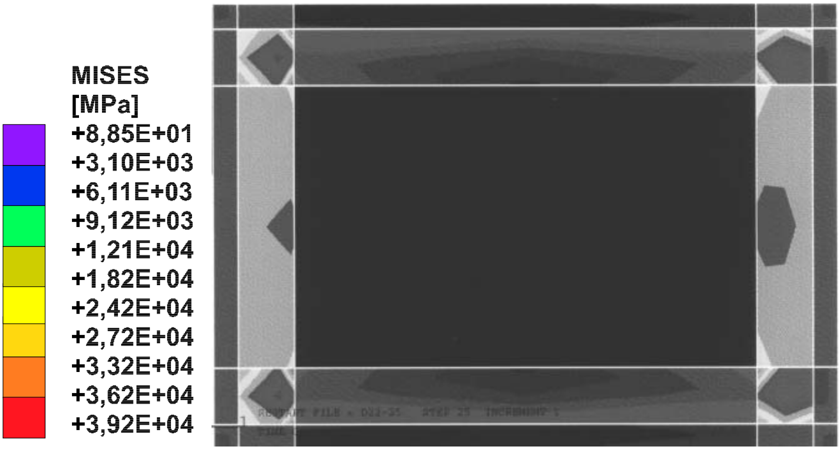

Figure 3.10. The equivalent stress σ_{22}^{eq} distribution in the RVE

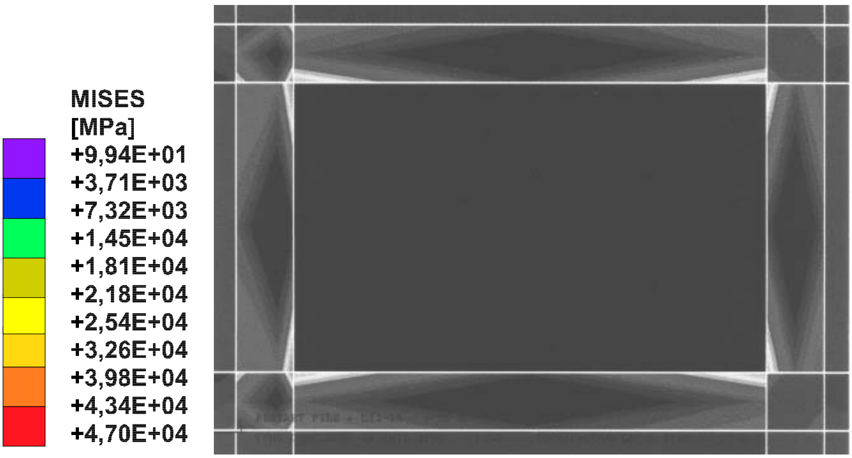

Figure 3.11. The equivalent stress σ_{12}^{eq} distribution in the RVE

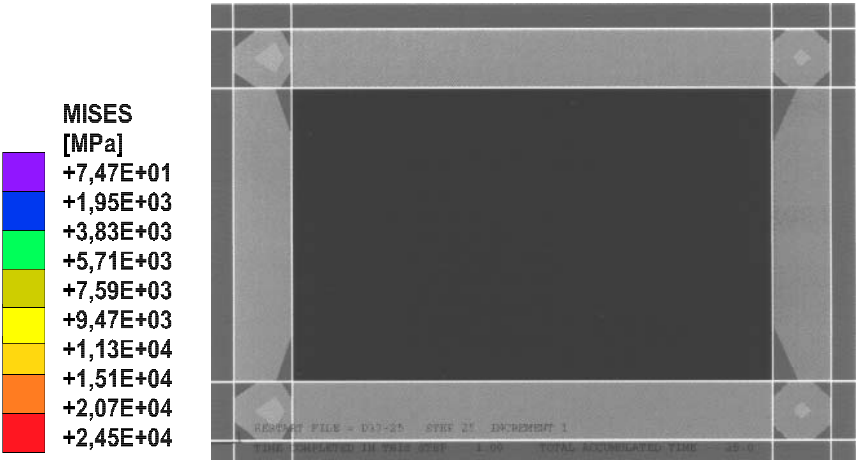

Figure 3.12. The equivalent stress σ_{33}^{eq} distribution in the RVE

That is why the FEM mesh should employed the most precisely around all interfaces – its density along the external RVE edges does not need to be so precise. Comparing the stresses fields spatial variations with analogous results collected in Sec. 2.3.3.2 it is seen that maximum stresses variations are obtained along the interface in RVE. This observation does not depend on the homogenisation approach used as well as on its FEM solution, so it is common for various cell problem solutions.

Further, the effective properties of the homogenised material are computed starting from the properties of the composite constituents and the constitutive relation verified for all strain increments during the computational incremental analysis. We use the relation (3.70) and therefore

$$C^{el} = \begin{bmatrix} k+\mu & k-\mu & k-\mu & 0 \\ k-\mu & k+\mu & k-\mu & 0 \\ k-\mu & k-\mu & k+\mu & 0 \\ 0 & 0 & 0 & \mu \end{bmatrix} = \begin{bmatrix} 15776.83 & 2601.7 & 2601.7 & 0 \\ 2601.7 & 15776.83 & 2601.7 & 0 \\ 2601.7 & 2601.7 & 15776.83 & 0 \\ 0 & 0 & 0 & 6587.57 \end{bmatrix}$$

while the inelastic part of the effective constitutive tensor can be written as

$$\mathbf{C}^{inel} = \sigma : \varepsilon^{-1} \rightarrow \mathbf{C}^{inel} = \begin{bmatrix} 3393.88 & 1505.92 & 2080.0 & 0 \\ 749.44 & 2653.36 & 1576.12 & 0 \\ 1631.4 & 1546.4 & 5017.2 & 0 \\ 0 & 0 & 0 & 499.600 \end{bmatrix},$$

which completes the calculations of the effective elastoplastic characteristics of the composite considered. As it is shown here, the homogenisation technique presented can be very efficiently used in case of linear elastic constituents of the composite. It can be used instead of the previous method, where the symmetry conditions have been applied on the external edges of the RVE and some specific stress boundary conditions were applied on the bimaterial (or multimaterial) interfaces.

3.5 Some Comments on Probabilistic Effective Properties

Deterministic approaches to homogenisation of elastoplastic or viscoelastoplastic composites worked out recently are more complicated than the analysis presented above. However some authors presented simplified approximations for the effective yield stresses or yield conditions. It is known that for some special case where the volume fractions of the fibre−matrix constituents are equal or almost equal, the effective yield stresses can be described as

$$\Sigma^{(eff)} = \sqrt{\Sigma_1 \Sigma_2} \tag{3.75}$$

where Σ_1, Σ_2 denote the yield stresses for the two−component composite. This relation is used to show how to calculate the probabilistic moments in case, where yield stresses are characterized by their first two probabilistic moments. These parameters are defined for fibre and matrix using $E[\Sigma_1]$, $\sigma(\Sigma_1)$ and $E[\Sigma_2]$, $\sigma(\Sigma_2)$. Considering the above, then the first two probabilistic moments of the effective parameter can be calculated starting from

$$\left(\Sigma^{(eff)}\right)^2 = \Sigma_1 \Sigma_2 \tag{3.76}$$

and by using the second order perturbation method, we get

$$\begin{aligned} & E\left[\left(\Sigma^{(eff)}\right)^2\right] \\ & = \int_{-\infty}^{+\infty} \left(\Sigma_2^0 + \varepsilon \Delta b_u \Sigma_2^{;u} + \tfrac{1}{2}\varepsilon^2 \Delta b_u \Delta b_v \Sigma_2^{;uv}\right) p_R(\mathbf{b}(x))\, d\mathbf{b} \\ & \times \int_{-\infty}^{+\infty} \left(\Sigma_1^0 + \varepsilon \Delta b_r \Sigma_1^{;r} + \tfrac{1}{2}\varepsilon^2 \Delta b_r \Delta b_s \Sigma_1^{;rs}\right) p_R(\mathbf{b}(x))\, d\mathbf{b} \\ & = E[\Sigma_1] E[\Sigma_2] \end{aligned} \tag{3.77}$$

since the second order derivatives of the effective yield stresses are equal to 0. Then, omitting second order terms being equal to 0, the variance of effective yield stresses can be calculated as

$$\begin{aligned} Var\left(\left(\Sigma^{(eff)}\right)^2\right) &= Var(\Sigma_1\Sigma_2) = \int_{-\infty}^{+\infty} \left(\Sigma_1\Sigma_2 - E[\Sigma_1\Sigma_2]\right) p_R(\mathbf{b}(x))\, d\mathbf{b} \\ &= \int_{-\infty}^{+\infty} \left\{ \left(\Sigma_1^0 + \varepsilon\Delta b_r \Sigma_1^{;r}\right)\left(\Sigma_2^0 + \varepsilon\Delta b_s \Sigma_2^{;s}\right) - \Sigma_1^0\Sigma_2^0 \right\} p_R(\mathbf{b}(x))\, d\mathbf{b} \\ &= Var^2(\Sigma_1) + Var^2(\Sigma_2) \end{aligned} \tag{3.78}$$

which gives a combination of variances under the assumption of uncorrelation of the variables Σ_1 and Σ_2. Finally, the expected value and variance of the effective yield stress can be determined from the following equation system:

$$E\left[\left(\Sigma^{(eff)}\right)^2\right] = E^2\left[\Sigma^{(eff)}\right] + Var\left(\Sigma^{(eff)}\right) \tag{3.79}$$

and

$$Var\left(\left(\Sigma^{(eff)}\right)^2\right) = 2Var\left(\Sigma^{(eff)}\right)\left(2E^2\left[\Sigma^{(eff)}\right] + Var\left(\Sigma^{(eff)}\right)\right) \tag{3.80}$$

Probabilistic moments of effective yield stresses of a composite can be found as a solution of (3.77) and (3.78) in conjunction with the statements (3.79) and (3.80). For illustration, using a matrix built up with the following material data: $E[\Sigma_2] = 80\ MPa$, $\sigma(\Sigma_2) = 8.0\ MPa$ and the fibre as $E[\Sigma_1] = 4100\ MPa$, $\sigma(\Sigma_1) = 410\ MPa$, the effective plastic stress is obtained as the expected value $E[\Sigma^{(eff)}] = 552.969\ GPa$ and the standard deviation $\sigma\left(\Sigma^{(eff)}\right) = 40.367\ GPa$.

3.6 Conclusions

As is shown in the computational experiments, the homogenised material obtained as a result of the Transformation Field Analysis (TFA) is stiffer in the nonlinear range than the original composite. It is caused by the fact that the constitutive relations during the whole iteration procedure are based on constant constitutive tensors $\mathbf{C}_r$ with elastic properties. To obtain a better effective approximation of composite behaviour, these matrices should be divided into elastic and plastic parts, after yielding, by means of the consistent tangent matrices.

Since the Transformation Field Analysis makes it possible to characterise explicitly the effective elastoplastic behaviour starting from composite component material properties, it is possible to carry out the numerical sensitivity studies of homogenised composite properties with respect to its original material characteristics. Such computational studies make it possible to determine the most decisive material parameter for the overall elastoplastic behaviour of the composite, which may be important in the context of optimisation techniques applied in composite engineering design studies.

Due to the fact that most of the composite components material characteristics are obtained experimentally as statistical estimators, the next step to utilise the present approach is probabilistic implementation of the homogenisation problem. It will generally enable us to compute the respective probabilistic moments and coefficients of effective properties, starting from the expected values and standard deviations of composite component elastoplastic characteristics. As is known, it can be done using the Monte Carlo simulation technique, for instance. Further, it should be mentioned that such an implementation makes it possible to specify the stochastic sensitivity of composite effective characteristics to the randomness of the component material nonlinear behaviour.

3.7 Appendix

The two-component transversely isotropic RVE of volume Ω is subjected to a uniform overall strain increment $\Delta\mathbf{E}$ or stress $\Delta\Sigma$. A possible description of the local uniform strain and stress increment field is suggested as

$$\Delta\varepsilon_r = \mathbf{A}_r \Delta\mathbf{E},\ r=1,2 \tag{A3.1}$$

$$\Delta\sigma_r = \mathbf{B}_r \Delta\Sigma,\ r=1,2 \tag{A3.2}$$

with further relations

$$c_1\mathbf{A}_1 + c_2\mathbf{A}_2 = \mathbf{I} \tag{A3.3}$$

$$c_1\mathbf{B}_1 + c_2\mathbf{B}_2 = \mathbf{I} \tag{A3.4}$$

Further, the local and overall increments are expressed as

$$\Delta\Sigma = c_1\Delta\sigma_1 + c_2\Delta\sigma_2 \quad \text{and} \quad \Delta\mathbf{E} = \mathrm{c}_1\Delta\varepsilon_1 + \mathrm{c}_2\Delta\varepsilon_2 \tag{A3.5}$$

with composite constituent volume fractions

$$c_1 = \frac{\Omega_1}{\Omega},\ c_2 = \frac{\Omega_2}{\Omega} \text{ and } \Omega_1 \cup \Omega_2 = \Omega\,. \tag{A3.6}$$

The constitutive relations for composite constituents in elastoplastic range are defined as

$$\Delta\sigma_r = \mathbf{C}_r \Delta\varepsilon_r\,, \quad \Delta\varepsilon_r = \mathbf{M}_r \Delta\sigma_r \quad \text{and} \quad \mathbf{M}_r = \mathbf{C}_r^{-1} \tag{A3.7}$$

while the overall properties are

$$\Delta\Sigma = \mathbf{C}\Delta\mathbf{E}\,, \quad \Delta\mathbf{E} = \mathbf{M}\Delta\Sigma \quad \text{and} \quad \mathbf{M} = \mathbf{C}^{-1} \tag{A3.8}$$

The constitutive and compliance matrices are given as the relevant spatial averages over the RVE

$$\mathbf{C} = \sum_{\mathrm{r=1}}^{2} \mathrm{c_r} \mathbf{C}_r \mathbf{A}_r\,, \quad \mathbf{M} = \sum_{\mathrm{r=1}}^{2} \mathrm{c_r} \mathbf{M}_r \mathbf{B}_r \tag{A3.9}$$

The individual components of $\mathbf{B}_r$ and $\mathbf{A}_r$ may be found as solutions of (A3.3) and (A3–4). There holds that

$$\mathbf{A}_r = \begin{bmatrix} 0.5(\mathrm{k/k_r} + \mu/\mu_r) & 0.5(\mathrm{k/k_r} - \mu/\mu_r) & 0.5(1\text{-}1_\mathrm{r})/k_r & 0 \\ 0.5(\mathrm{k/k_r} - \mu/\mu_r) & 0.5(\mathrm{k/k_r} + \mu/\mu_r) & 0.5(1\text{-}1_\mathrm{r})/k_r & 0 \\ 0 & 0 & 1 & 0 \\ 0 & 0 & 0 & \mu/\mu_r \end{bmatrix} \tag{A3.10}$$

as well as

$$\mathbf{B}_r = \frac{1}{E_C} \begin{bmatrix} E_C & 0 & 0 & 0 \\ 0 & E_C & 0 & 0 \\ (1-c_r)a_r & (1-c_r)a_r & E_{rL} & 0 \\ 0 & 0 & 0 & E_C \end{bmatrix}, \text{ for } r=1,2 \tag{A3.11}$$

where

$$E_C = c_1 E_{(1)L} + c_2 E_{(2)L} \quad \text{and} \quad a_1 = \left(\nu_{(1)L} E_{(2)L} - \nu_{(2)L} E_{(1)L}\right) = -a_2 \tag{A3.12}$$

Next, the transformation and concentration matrices $\mathbf{D}_{rs}$, $\mathbf{F}_{rs}$ are calculated as

$$\mathbf{D}_{r1} = (\mathbf{I} - \mathbf{A}_r)(\mathbf{C}_1 - \mathbf{C}_2)^{-1}\mathbf{C}_1\,, \quad \mathbf{D}_{r2} = (\mathbf{I} - \mathbf{A}_r)(\mathbf{C}_1 - \mathbf{C}_2)^{-1}\mathbf{C}_2 \tag{A3.13}$$

$$\mathbf{F}_{r1} = (\mathbf{I} - \mathbf{B}_r)(\mathbf{M}_1 - \mathbf{M}_2)^{-1}\mathbf{M}_1\,, \quad \mathbf{F}_{r2} = (\mathbf{I} - \mathbf{A}_r)(\mathbf{M}_1 - \mathbf{M}_2)^{-1}\mathbf{M}_2 \tag{A3.14}$$

with $\mathbf{D}_{11}$, $\mathbf{D}_{12}$, $\mathbf{D}_{21}$, $\mathbf{D}_{22}$, $\mathbf{F}_{11}$, $\mathbf{F}_{12}$, $\mathbf{F}_{21}$, $\mathbf{F}_{22}$ to be calculated. The components of the matrix $\mathbf{D}_{11}$ are obtained as, for instance,

$$\mathbf{D}_{11} = \begin{bmatrix} D_{1111} & D_{1112} & D_{1113} & D_{1114} \\ D_{1121} & D_{1122} & D_{1123} & D_{1124} \\ D_{1131} & D_{1132} & D_{1133} & D_{1134} \\ D_{1141} & D_{1142} & D_{1143} & D_{1144} \end{bmatrix} \tag{A3.15}$$

then

$$D_{1111} = \left(1 - \frac{k}{2k_1} - \frac{\mu}{2\mu_1}\right)(2k_1 + l_1) \times \left[\frac{2l_1(k_1 - k_2) + 2l_2(k_2 - k_1) + (k_1 - k_2)^2 + (\mu_1 - \mu_2)^2}{\left((k_1 - k_2)^2 + (\mu_1 - \mu_2)^2\right)(l_1 - l_2)}\right] \tag{A3.16}$$

$$D_{1112} = \left(1 - \frac{k}{2k_1} + \frac{\mu}{2\mu_1}\right)(2k_1 + l_1) \times \left[\frac{2l_1(k_1 - k_2) + 2l_2(k_2 - k_1) + (k_1 - k_2)^2 + (\mu_2 - \mu_1)^2}{\left((k_1 - k_2)^2 + (\mu_2 - \mu_1)^2\right)(l_1 - l_2)}\right] \tag{A3.17}$$

$$D_{1113} = \left[1 - \frac{k_1}{2}(l - l_1)\right](2l_1 + n_1)\left[\frac{l_1 - l_2 + 2(n_1 - n_2)}{(l_1 - l_2)(n_1 - n_2)}\right] \tag{A3.18}$$

$$D_{1121} = \left(1 - \frac{k}{2k_1} + \frac{\mu}{2\mu_1}\right)(2k_1 + l_1) \times \left[\frac{2l_1(k_1 - k_2) + 2l_2(k_2 - k_1) + (k_1 - k_2)^2 + (\mu_2 - \mu_1)^2}{\left((k_1 - k_2)^2 + (\mu_2 - \mu_1)^2\right)(l_1 - l_2)}\right] \tag{A3.19}$$

$$D_{1122} = \left(1 - \frac{k}{2k_1} - \frac{\mu}{2\mu_1}\right)(2k_1 + l_1) \times \left[\frac{2l_1(k_1 - k_2) + 2l_2(k_2 - k_1) + (k_1 - k_2)^2 + (\mu_1 - \mu_2)^2}{\left((k_1 - k_2)^2 + (\mu_1 - \mu_2)^2\right)(l_1 - l_2)}\right], \tag{A3.20}$$

$$D_{1123} = \left[1 - \frac{k_1}{2}(l - l_1)\right](2l_1 + n_1)\left[\frac{l_1 - l_2 + 2(n_1 - n_2)}{(l_1 - l_2)(n_1 - n_2)}\right] \tag{A3.21}$$

$$D_{1144} = \mu_1\left(1 - \frac{\mu}{\mu_1}\right)\left(\frac{1}{\mu_1 - \mu_2}\right) \tag{A3.22}$$

The remaining coefficients of $\mathbf{D}_{11}$ are equal to 0.